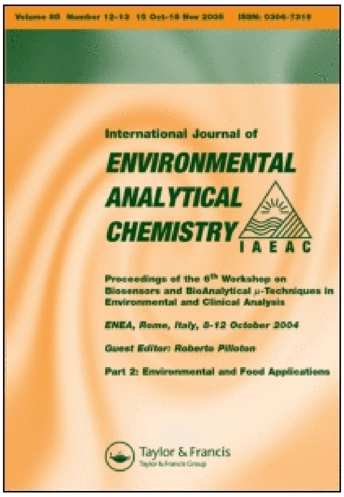

International Journal of Environmental Analytical Chemistry
Publication details, including instructions for authors and subscription information:
http://www.informaworld.com/smpp/title~content=t713640455

Sedimentary process inferences from Humic substances analysis and deposition rates (Western Ross Sea, Antarctica)

Nicoletta Calace[a]; Federico Giglio[b]; Sabrina Mirante[a]; Bianca Maria Petronio[a]; Mariangela Ravaioli[b]
[a] Dipartimento di Chimica, Università "La Sapienza" di Roma, P.le A. Moro 5, 00185 Rome, Italy [b] Istituto di Geologia Marina, Via P. Gobetti 101 40129 Bologna, Italy

To cite this Article Calace, Nicoletta , Giglio, Federico , Mirante, Sabrina , Petronio, Bianca Maria and Ravaioli, Mariangela(2004) 'Sedimentary process inferences from Humic substances analysis and deposition rates (Western Ross Sea, Antarctica)', International Journal of Environmental Analytical Chemistry, 84: 6, 423 — 439

To link to this Article: DOI: 10.1080/03067310310001637658

URL: http://dx.doi.org/10.1080/03067310310001637658

Intern. J. Environ. Anal. Chem.
Vol. 84, Nos. 6–7, pp. 423–439, 15 May–15 June 2004

Taylor & Francis
Taylor & Francis Group

SEDIMENTARY PROCESS INFERENCES FROM HUMIC SUBSTANCES ANALYSIS AND DEPOSITION RATES (WESTERN ROSS SEA, ANTARCTICA)

NICOLETTA CALACE[a], FEDERICO GIGLIO[b], SABRINA MIRANTE[a],
BIANCA MARIA PETRONIO[a,*] and MARIANGELA RAVAIOLI[b]

[a]*Dipartimento di Chimica, Università "La Sapienza" di Roma, P.le A. Moro 5, 00185 Rome, Italy;*
[b]*Istituto di Geologia Marina, Via P. Gobetti 101 40129 Bologna, Italy*

(Received 25 October 2001; In final form 28 May 2003)

The first 40 cm of sediment of three basins in the Ross Sea were sampled using a box corer. Site Y1 was located close to the coast in Terra Nova Bay; the sediment of site Y3 was collected in a more distal basin in the central sector of the Ross Sea; finally site Y5 was sampled in the deepest zone of the Joides Basin.

Sediment cores were sliced and analysed with a depth resolution of 2–4.5 cm. The distribution of humic substances and their structural features along the cores were determined and related to the pattern of Total Organic Carbon (TOC) and sedimentological data. The grain size distribution and the ^{210}Pb inventories allow the sediment of the study sites to be characterised.

The humic substance content in the sediment decreases, with a change in slope between 23 and 26 cm at Y1, between 12 and 15 cm at Y3 and constant values with further depth. At Y5 the depth profile of humic substance content shows constant values in the upper 17 cm and values decrease with further depth. The pattern of humic substance yield is similar to that found for TOC. The analysis of the elemental composition of the humic acids extracted from different sediment depths shows an increasing C/N atomic ratio at sites Y1 and Y3 and constant values along the Y5 core. The depth profile of the C/N atomic ratio is confirmed by the changes observed in the structural characterisation and indicates a shift from the freshly deposited organic matter on the sediment surface to more humified material (humin). The results obtained highlight a different sedimentation rate at the three sites as deduced from sedimentological analysis.

Keywords: Humic substances; Total organic carbon; Elemental analysis; Grain size; Accumulation rate; Antarctica

INTRODUCTION

The organic matter in Antarctic seawater typically consists of a complex mixture of carbohydrates, proteins, lipids, and other compounds stemming from autochthonous sources. Although an important portion of this organic matter is degraded chemically and biologically inside the water column, a significant portion reaches the sediment

---

*Corresponding author. Fax: +39-064-9913723. E-mail: biancamaria.petronio@uniroma1.it

ISSN 0306-7319 print: ISSN 1029-0397 online
DOI: 10.1080/0306731031001637658

surface where it is subjected to further chemical and biological transformations. The organic matter degrades over timescales covering ten orders of magnitude, ranging from minutes for the breakdown of biochemicals sourced from algae and organisms death in coastal sediments to 10^6 years for mineralisation in deep-sea sediments [1]. However, not all sedimentary organic matter degrades, and a portion of organic carbon is found in ancient sediments. This finding is due to preservation mechanisms involving some kinds of organic macromolecules [2–6].

Some authors [7–10] have pointed out that some sterols, polyphenolic macromolecules and proteinaceous material are entrapped by means of adsorption/protection mechanisms in the sediments generating the organic carbon reservoir. Nevertheless, a large part of the preserved organic matter consists of molecularly uncharacterised components.

The humic substances represent a class of these molecularly uncharacterised compounds and are intermediate products in a humification process which proceeds as far as the formation of humin (highly refractory product [11]). The microbial activities and chemical processes occurring in anoxic conditions are responsible for the formation of humic substances, which, according to the biotic-condensation and the biopolymer-degradation models, involves both polymerisation and degradation [12–15]. The degradation is actually considered to be a preliminary stage or even a prerequisite for polymerisation [16] even if the formation of humic substances in sediments is still under debate [13].

Sediment accumulation rate and grain size are the environmental variables most commonly believed to have an effect on the reactivity and ultimate preservation of organic matter [2]. Rapid deposition moves organic matter down through diagenetically active zones (surface sediment where more electron acceptors are present) and it leads to a high degree of preservation. The sediment accumulation rate is usually related to organic matter bulk even if this correlation is subject to variations due to different inputs of organic debris, bioturbation, etc. On the other hand, sediment grain size might also be related to the reactivity and preservation of sedimentary organic matter on the basis of organic matter adsorption mechanisms.

In this paper, we discuss a new utilisation of the humic substances, which represent a fraction of preserved sedimentary organic matter, as a marker of the accumulation conditions. Radiotracers such as ^{210}Pb and grain size analyses are utilised to support the sedimentary conclusion obtained via a biochemical approach.

STUDY AREA

The western Ross continental shelf has an average depth of around 500 m and slopes towards the continent. It is characterised by a series of elongated banks running northeast (*ca.* 300 m) and basins ($>$ 500 m; Fig. 1). It is an extremely rugged and deep area [17], particularly near the Victoria Land coast, where outlet glaciers have eroded the seafloor and created narrow transverse troughs as deep as 1200 m close to the continent. The irregular topography of the western Ross Sea shelf is further emphasised by the volcanic islands and seamounts of the McMurdo Sound complex that extend along a roughly north–south line from McMurdo Sound to Cape Adare.

The three study sites located along the east–west transect, from the coast to the open sea in the marginal ice zone of the Ross Sea continental shelf (Fig. 1) were chosen on the

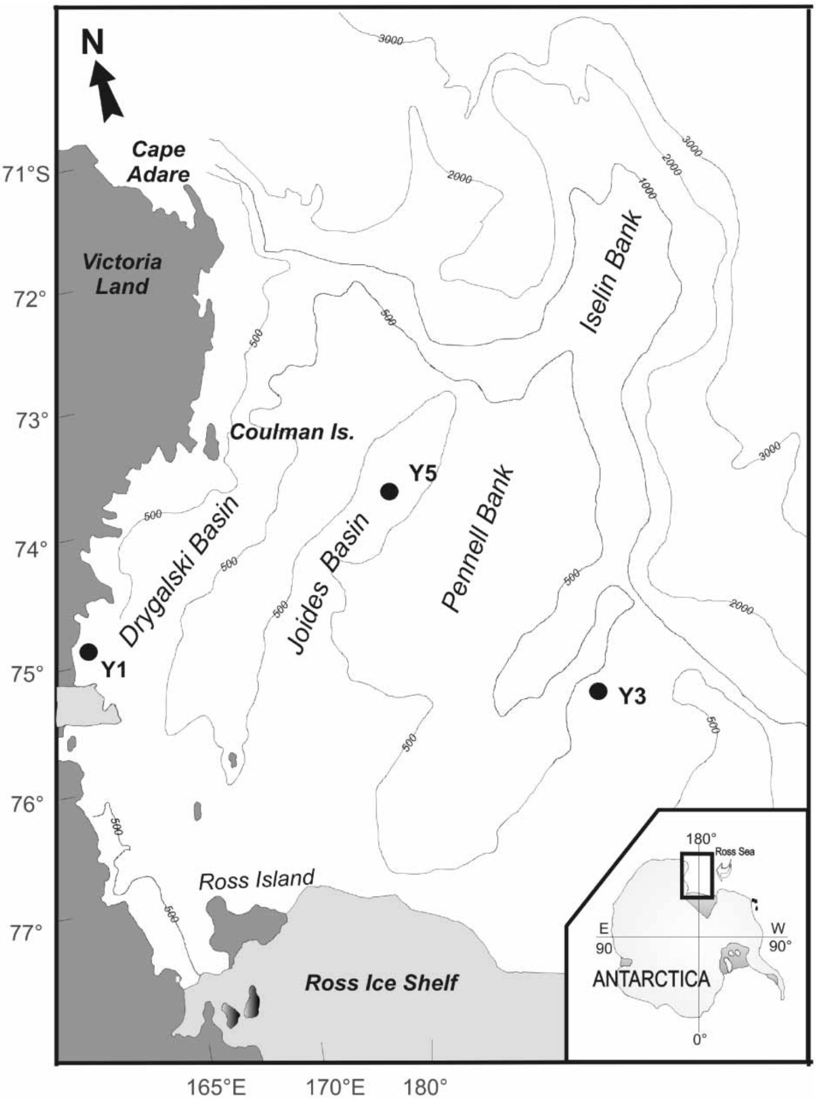

FIGURE 1 Map of sampling sites.

basis of the temperature, dissolved oxygen and salinity profiles characterizing the water column, in order to study particle fluxes through the water column using moored instruments (sediment traps, current meters and a transmissometer). Site Y1 (75° 04′ S, 164° 13′ E) was located in the western Ross Sea at a depth of 950 m close to Terra Nova Bay, on the southern flank of the Drygalsky basin. This area is representative of an environment with high energy and reworked sediment [18]. Material was collected at a depth of 628 m at site Y3 (75° 54′ S, 177° 34′ W), in an area near the continental shelf break in a central Ross Sea basin. The study of this area is instrumental in an understanding the dynamics of the Ice-Shelf waters in the Ross Sea hydrological system. Finally site Y5 (74° 00′ S, 174° 48′ E), located in the centre of the northern part of the Joides Basin at a depth of 582 m, represents a setting characterised by high biosiliceous sediment accumulation [18].

EXPERIMENTAL

Sampling

Sediments were sampled using a box corer during the 1997/98 Italian Antarctic Expedition. Several cores were recovered from the same box core for different analyses. One of these cores (40 cm) was immediately subdivided into fourteen layers (Table I) in order to obtain a high-depth resolution in the organic matter and humic substance analyses. The layers were then frozen to −30°C and processed within one year. The decision to use different thicknesses for the measured layers arose from the different accumulation rates measured in the same areas in a previous study, so that a similar time resolution was obtained.

One other core was X-rayed using a Girardoni M60 tube and an aluminium and PVC filter, scanned for magnetic susceptibility and then split into two parts. After visual examination the core was sub-sampled at a resolution of 2 cm for the purpose of radiochemical and grain-size analysis. Bulk density was calculated from sediment porosity, assuming a particle density of 2.5 g cm^{-3}.

Extraction of Humic Substances

The classical method of solubility-based fractionation [19] was used to isolate humic substances. Sediment samples (200 g of wet sediment) were alternatively batched three times with 2 L HCl (0.1 M) and with 2 L NaOH (0.5 M) in polyethylene vessels for 24 h on an Intercontinental rotary shaker model DRM06020. The acid extract was eliminated and the alkaline extract separated from the insoluble residue (humins and inorganic components) by centrifugation (3000 × *g* for 20 min) with a Vismara

TABLE I Thickness of layers obtained by subdividing the sediment cores

Layer	*Thickness (cm)*		
	Y1	*Y3*	*Y5*
1	0–2.5	0–2	0–2
2	2.5–5	2–4.5	2–4
3	5–7.5	4.5–7	4–6
4	7.5–10	7–10.5	6–8
5	10–12.5	10.5–13	8–10
6	12.5–15	13–15.5	10–12.5
7	15–17.5	15.5–17.5	12.5–15
8	17.5–20	17.5–20.5	15–17.5
9	20–23	20.5–23.5	17.5–20
10	23–26	23.5–27.5	20–23
11	26–29	27.5–32.5	23–26
12	29–32	32.5–36.5	26–29
13	32–36	36.5–40	29–32
14			32–36

centrifuge model 3225R. After acidification with concentrated HCl to pH 2, the humic acids were allowed to precipitate for 24 h at 25°C and separated from the acid-soluble supernatant (containing fulvic acids) by centrifugation ($3000 \times g$ for 45 min). Before freeze-drying with a Labconco lyophiliser model 77 400, the humic acids were purified by means of dialysis against deionised water using tubular membranes (Spectra/Por®) with a molecular weight size of 1000 Da. The fulvic acids were recovered from the supernatant acid and purified by passing over an Amberlite XAD-8 resin column according to a published method for the extraction of aquatic humic substances [20,21].

All reagents are analytical RPE grade from Carlo Erba.

Total Organic Carbon

The Total Organic Carbon (TOC) content of the sediment was determined using a Carlo Erba model EA11110 CHNS-O Element Analyser. 100 mg of dried sediment was acidified with 500 μL of concentrated HCl in order to eliminate the carbonate fraction, then freeze-dried and reweighed. The freeze-dried residue was then analysed for TOC. The measurements were repeated six times and the relative standard deviations were less than 5%.

Chemical and Spectroscopic Analyses

The carbon, hydrogen, nitrogen and sulphur content of the humic substances was determined with the instrument used for TOC. Samples for Fourier Transform Infra-Red (FTIR) spectroscopy were prepared by mixing 1 mg of the humic acid with 100 mg of oven-dried KBr (110°C). The spectra were recorded using a Philips model PU9800 FTIR spectrophotometer working in diffuse reflectance conditions. Reflectance spectra were converted to Kubelka Munk units, which are directly proportional to the concentration of the scattering medium. 100 scans were recorded with a resolution of 4 cm^{-1} and normal apodisation.

^{13}C-NMR spectra were determined in 0.5 M NaOD by a Varian spectrometer, model XL-300. Samples were prepared by dissolving the dried residue (30 mg) in 1 mL of NaOD in an NMR tube (5 mm). The operating conditions were: 75 MHz, pulse 45°, acquisition time 0.1 s, delay time 0.5 s. About 800 000 scans were accumulated. Spectra were performed in broadband decoupling mode. Under these conditions, a clear spectrum should be obtained with distinct single peaks for each carbon atom; because of the molecular complexity of samples, the spectra show many poorly resolved signals.

Thermogravimetric analyses of humic substances were carried out using a Perkin-Elmer TGA7 thermobalance. The samples were heated from 50 to 1300°C at a rate of 10°C min^{-1} under nitrogen atmosphere.

Grain Size and Radiochemical Analyses

Sediment samples were described for visible sedimentological characteristics and X-rayed; then grain size composition was obtained using common methods involving the use of sieves and an X-ray sedigraph.

α-Particle counting of ^{210}Po was used for ^{210}Pb determinations, assuming secular equilibrium between the two isotopes. Up to 3.0 g of dry sediment was leached with hot 8 N HNO_3 and 30% H_2O_2 after spiking with ^{208}Po tracer. ^{210}Po in the leaching solution was plated onto a silver disc after evaporation to a small volume, elimination of HNO_3 using concentrated HCl, dissolution in 60 mL of 1.5 N HCl, filtration and reduction of iron by adding ascorbic acid. For the determination of excess ^{210}Pb we assumed that supported ^{210}Pb activity in each core is constant [22].

Mass depths in cores were measured from sediment porosity assuming a particle density of 2.5 g cm^{-3}. Inventories were obtained by integrating the excess ^{210}Pb activity depth profile *vs.* mass depth. Expected excess ^{210}Pb inventories were calculated from the integrated production in the water column by ^{226}Ra decay (0.2 dpm L^{-1}) [23].

RESULTS

Total Organic Carbon and Humic Substances Profiles

The TOC content (Fig. 2a) shows a decrease with depth in site Y1 sediment cores, even if the data are characterized by high variability. At site Y3 the depth profile of TOC (Fig. 2b) shows a slight decrease down to 20 cm and then constant values at greater depths. In the sample from Y5 the depth profile of TOC (Fig. 2c) shows constant values in the upper 10 cm which then decrease with increasing depth.

The humic acid content in the sediment decreases, with a change in slope between 23 and 26 cm at Y1 (Fig. 3a), between 12 and 15 cm at Y3 (Fig. 3b) and constant values with further depth. At Y5 the depth profile of humic acid content (Fig. 3c) shows constant values in the upper 17 cm and decreased values with further depth. The Y5 sediment core has the highest humic acid content (3.4 mg g^{-1}) down to 17 cm. The Y3 sediment core shows the lowest humic acid content which decreases from 1.8 to 0.4 in the upper 12 cm in depth. The Y1 sediment core shows a similar pattern to Y3 but with a higher humic acid content.

The fulvic acid content (Fig. 3a,b,c) pattern is practically the same as for humic acids but the amounts of fulvic acids are lower than those of humic acids.

Structural Characterisation of Humic Substances

Depth-related analysis of the elemental composition of the humic acids extracted from different sediment depths shows an increase in carbon content and a decrease in nitrogen content in a downward direction (Table II). The results for single elements are reflected in an increasing C/N atomic ratio. The increase of C/N atomic ratio (Fig. 4) is evident at sites Y1 and Y3. The C/N atomic ratios of humic acids extracted from the Y5 core are roughly constant (Fig. 4).

The H/C atomic ratio values also have a constant pattern at site Y5 while they decrease slightly with depth at sites Y1 and Y3 (Table II). The H/C ratio values indicate the relationship between the aliphatic and aromatic components of the humic acids.

FTIR spectra of humic acids extracted from the surface layer at the three sites (Fig. 5a) showed similar structural features. The spectra displayed absorption bands, indicating the presence of peptides at 1690 (C=O stretching), 1540 (N–H deformation) and 1230 cm^{-1} (C–N deformation). Moreover, the spectra showed the typical signal

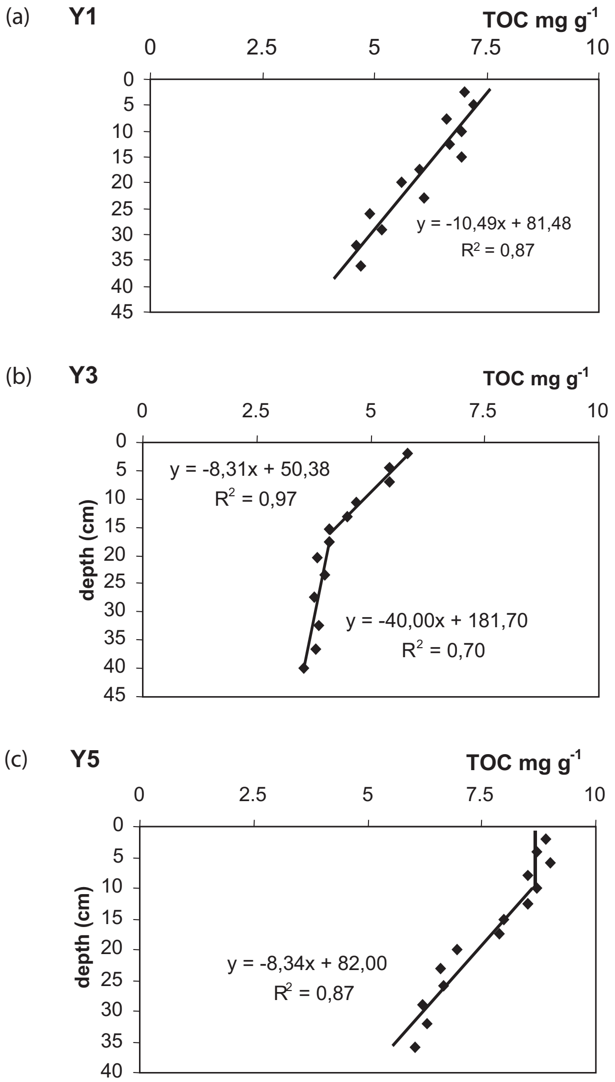

FIGURE 2 Total organic carbon profiles at sites (a) Y1, (b) Y3 and (c) Y5.

at 1040 cm^{-1} due to the C–O stretching of carbohydrates. At stations Y1 and Y3 (Fig. 5b), both the peptide and carbohydrate signals in the humic acids decreased with increasing depth. At station Y5 the spectra did not change with increasing depth. This result is consistent with the pattern of C/N and H/C ratios with depth.

^{13}C NMR spectra (Fig. 6) showed a wide range of resonance at 0–40 ppm due to the aliphatic carbon, which decreased with depth relative to the aromatic carbon resonance at 110–140 ppm in samples from sites Y1 and Y3. The results obtained from spectroscopic analysis confirmed those of elemental composition analysis.

Thermogravimetric analyses (Fig. 7) performed on humic acids extracted from surface layers at the three sites showed two weight losses. The first, in the temperature

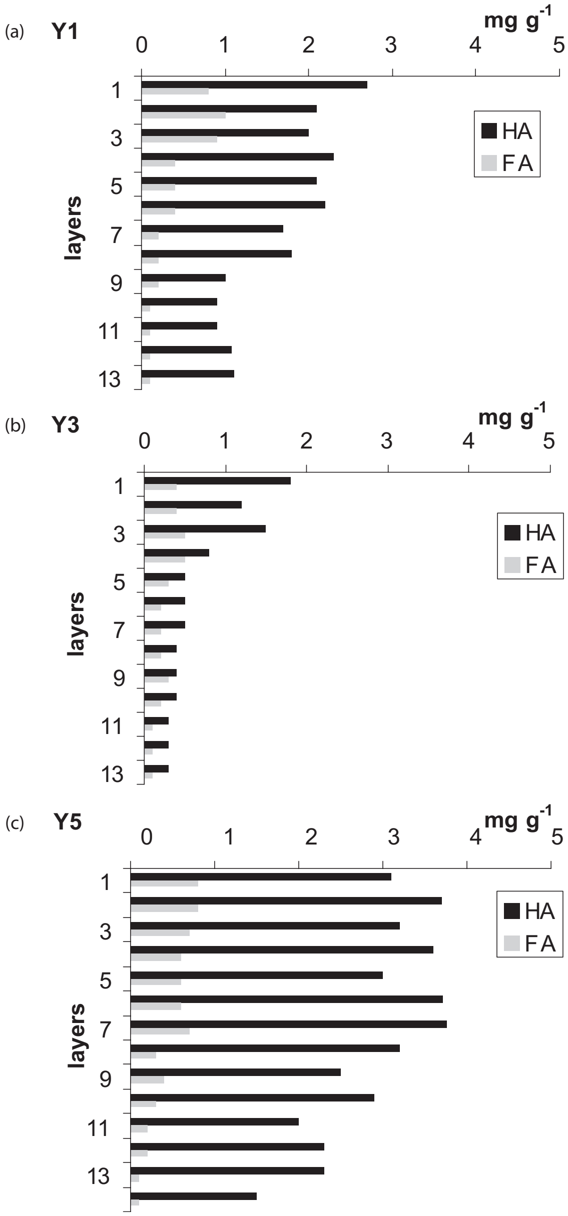

FIGURE 3 Humic and fulvic acid (mg g^{-1}) profiles at sites (a) Y1, (b) Y3 and (c) Y5.

range 150–350°C, is mainly due to the thermally labile component, while the second in the range 380–650°C is due to the thermo-resistant constituents. The thermal degradation of carbohydrate fragments, the decarboxylation of acid and/or amidic groups and the dehydration of hydroxylated aliphatic structures are the main reactions occurring below 350°C. The dissociation and breakdown of aromatic structures begins at 380–450°C; the decomposition and/or nuclear rearrangement of the polynuclear systems of humic acid molecules occurs above 450°C. The weight loss between

TABLE II The nitrogen and carbon content (%) of humic acids

Layer	*Y1*			*Y3*			*Y5*		
	N	*C*	*H/C*[a]	*N*	*C*	*H/C*[a]	*N*	*C*	*H/C*[a]
1	6.12 ± 0.06	50.51 ± 1.12	1.42	6.12 ± 0.08	50.51 ± 1.22	1.42	5.70 ± 0.09	51.70 ± 1.05	1.53
2	6.49 ± 0.03	56.20 ± 1.24	1.43	5.57 ± 0.04	52.59 ± 2.01	1.47	5.50 ± 0.09	48.70 ± 2.22	1.55
3	6.52 ± 0.11	57.92 ± 1.17	1.35	5.96 ± 0.07	53.80 ± 1.43	1.42	5.80 ± 0.08	54.20 ± 1.97	1.53
4	5.80 ± 0.06	52.55 ± 2.01	1.39	5.83 ± 0.07	55.73 ± 1.54	1.46	5.70 ± 0.11	54.30 ± 1.69	1.46
5	5.68 ± 0.12	54.52 ± 1.64	1.40	6.16 ± 0.11	53.91 ± 2.01	1.46	5.40 ± 0.13	57.20 ± 1.73	1.41
6	5.85 ± 0.09	57.65 ± 1.72	1.35	5.61 ± 0.08	54.45 ± 1.64	1.44	5.60 ± 0.08	55.40 ± 2.05	1.45
7	5.71 ± 0.07	56.45 ± 2.03	1,38	5.30 ± 0.04	51.85 ± 1.78	1.44	5.50 ± 0.09	56.80 ± 2.67	1.46
8	5.38 ± 0.11	57.56 ± 2.04	1.26	4.65 ± 0.06	56.86 ± 2.21	1.43	5.50 ± 0.14	56.80 ± 1.79	1.42
9	4.82 ± 0.11	56.75 ± 1.89	1.25	4.42 ± 0.03	57.29 ± 2.31	1.30	5.60 ± 0.11	57.20 ± 1.89	1.41
10	4.36 ± 0.04	59.04 ± 2.02	1.11	4.51 ± 0.03	58.05 ± 1.96	1.26	5.20 ± 0.12	56.50 ± 1.87	1.34
11	4.46 ± 0.07	55.30 ± 1.96	1.23	3.13 ± 0.02	56.50 ± 1.89	1.22	5.70 ± 0.08	57.01 ± 2.01	1.45
12	4.46 ± 0.05	57.02 ± 1.98	1.06	3.18 ± 0.02	56.68 ± 1.77	1.17	5.10 ± 0.06	56.80 ± 2.06	1..35
13	3.76 ± 0.07	58.04 ± 1.68	0.94	3.18 ± 0.03	56.60 ± 2.04	1.21	5.40 ± 0.07	56.80 ± 2.33	1.39
14							5.50 ± 0.04	57.70 ± 1.78	1.37

[a] The relative standard deviations are less than 3%.

150 and 350°C is 30–40% in humic acids extracted from surface layers and decreases by up to 20–25% in deeper samples. Conversely, the weight loss associated with thermo-resistant constituents (380–650°C) of humic macromolecules increases with depth, highlighting the fact that condensation reactions leading to a humic acid load occur more as depth increases.

Visual and X-ray Description and Grain-size Composition

At site Y5 the most evident lithologic features of sediments derived from visual descriptions and X-ray analyses show a strong bioturbation in the first 15 cm where benthic fauna is mainly composed of infauna sedimentary forms, mostly represented by polychaetes (77%), and crustacean peracarids (11.3%). Other groups, such as bivalve molluscs and echinoderms, are less represented [24,25].

The grain-size depth distribution in the box cores examined are shown in Fig. 8(a). At site Y5 the sediment is made up of fine materials consisting of siliceous mud and ooze without gravel. The sediment at sites Y1 and Y3 can be classified as siliceous mud with a gravel component in the second due to an input of ice-rafted debris. Y1 shows a coarser grain size, probably because a large contribution of continental material from the ice termination near the coast occurs in this zone [18].

^{210}Pb Distribution

^{210}Pb activity depth profiles are shown in Fig. 8(b). A surface mixed layer is clearly visible at site Y3 for about 7 cm. Below this layer the profile decreases with the expected exponential trend. Site Y5 shows some irregularities in the first 5 cm of the top sediment, and finally site Y1 is characterized by a regular exponential ^{210}Pb trend in depth. It is also important to note that the profiles attain equilibrium at different depths, similar for sites Y1 and Y3 (*ca.* 10 cm), while at Y5 equilibrium seems to occur at a deeper position (*ca.* 20 cm). Accumulation rates have been calculated

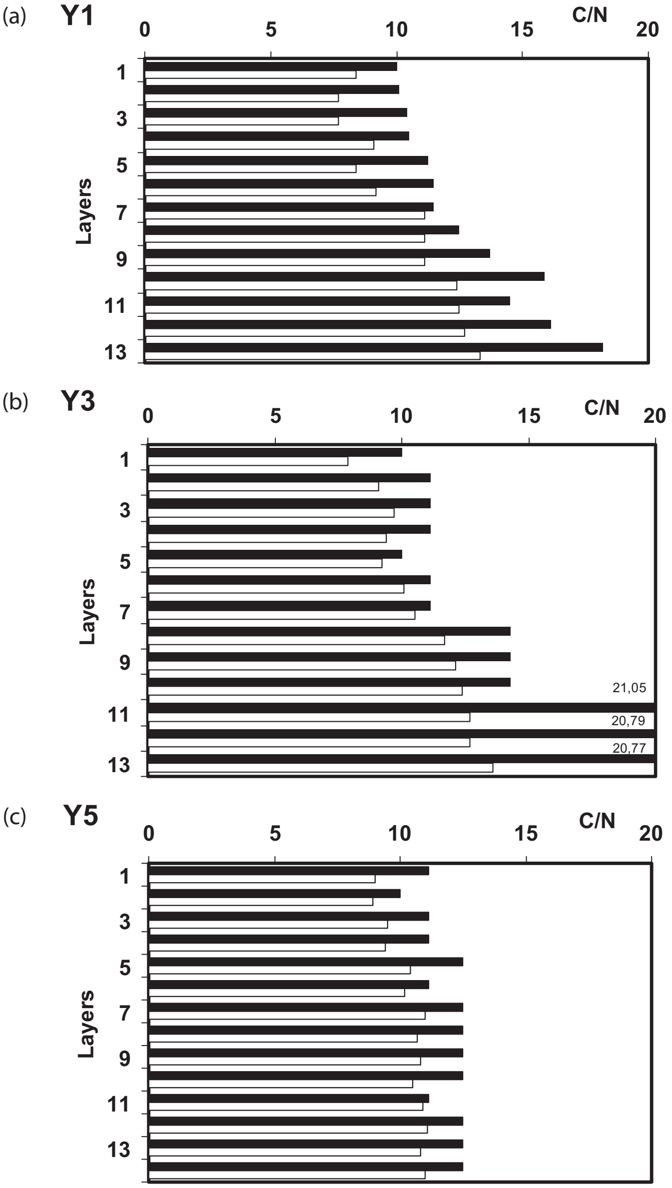

FIGURE 4 Profiles of atomic C/N ratio of humic and fulvic acids at sites (a) Y1, (b) Y3 and (c) Y5.

and discussed for all the sites studied. In any case we must always remember that accumulation rates calculated using ^{210}Pb can be subject to a substantial error due to mixing processes occurring in the area [23,26,27].

To determine the excess ^{210}Po, we assumed that supported ^{210}Pb activity is constant in each site. The value of supported ^{210}Pb was estimated from the total ^{210}Pb activity at the base of the box cores, where ^{210}Pb and ^{226}Ra were considered to be in radioactive equilibrium.

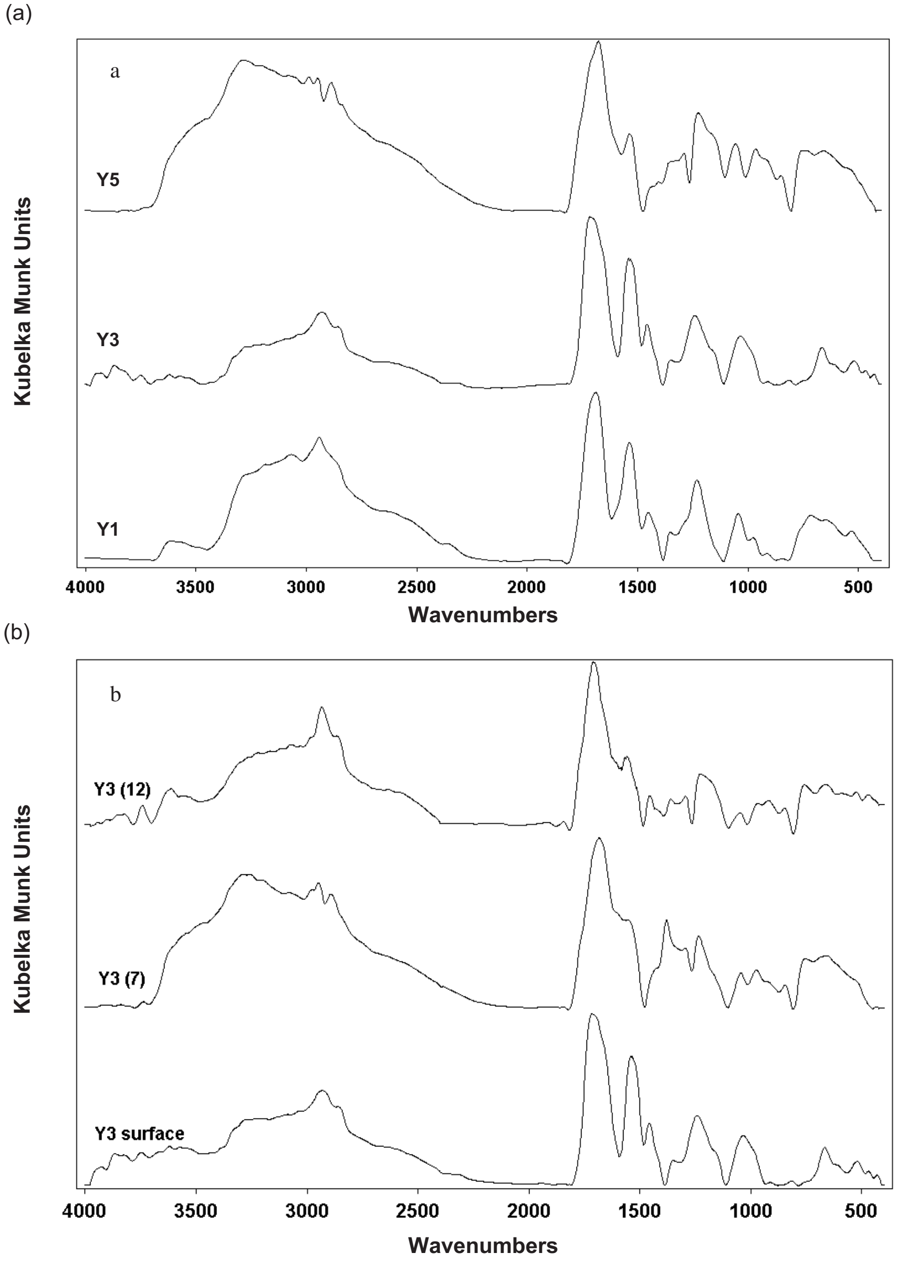

FIGURE 5 FTIR spectra of humic acids extracted from (a) the surface layers at all three sites and (b) the surface and layers 7 and 12 from site Y3.

DISCUSSION

Humic Substance Interpretation

The principal causes of the pattern of decreasing TOC as depth increases are normally microbial degradation and mineralisation processes. On the other hand, the

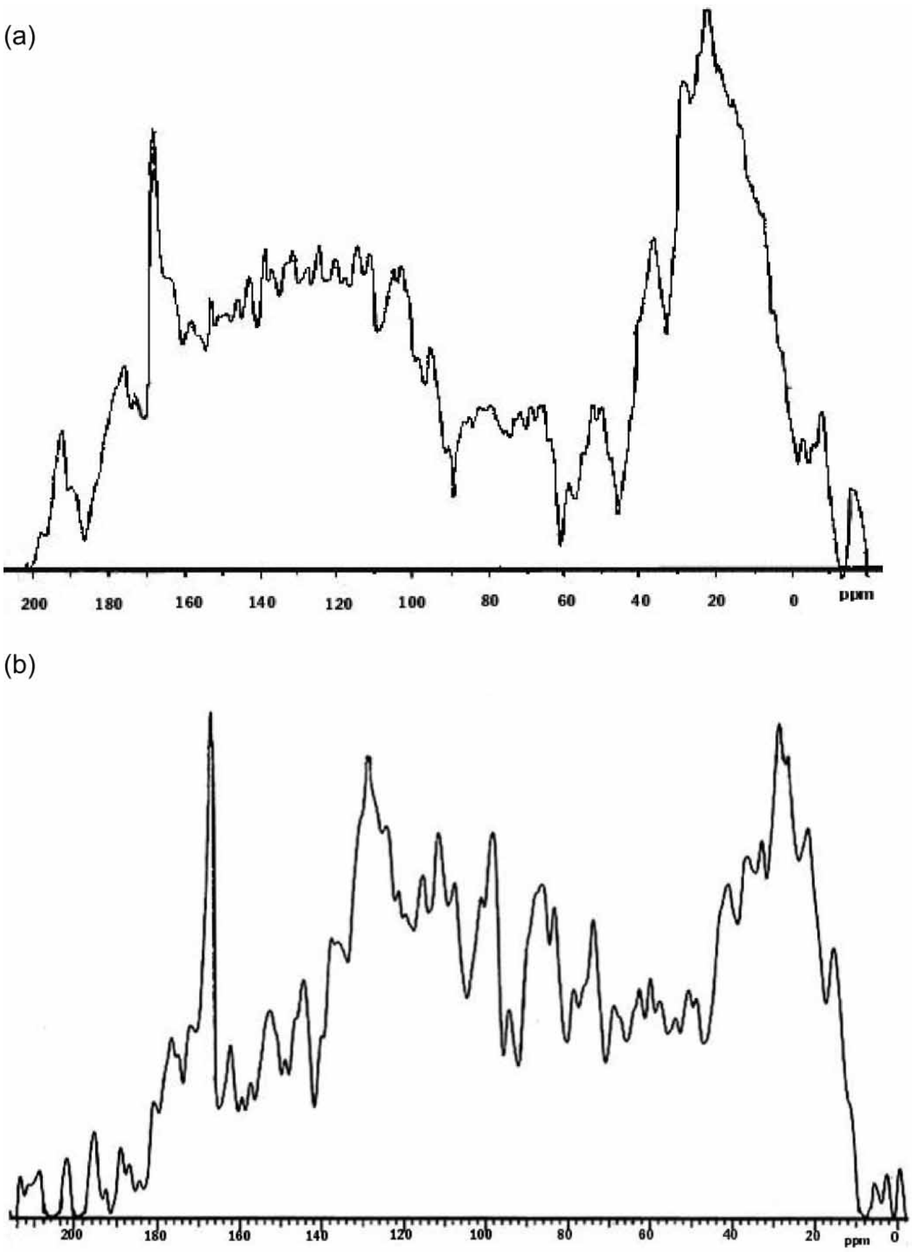

FIGURE 6 ^{13}C NMR spectra of humic acids extracted from (a) the surface layer and (b) the bottom layer of site Y3.

grain-size composition of sediment cores can also influence the organic carbon utilisation processes. Different researchers have pointed out [28–30] that a large fraction of organic matter in fine-grained siliciclastic aquatic sediments is associated with clay mineral particles, affecting the reactivity of organic matter during early diagenesis. In particular, the proteinaceous material and aromatic structures

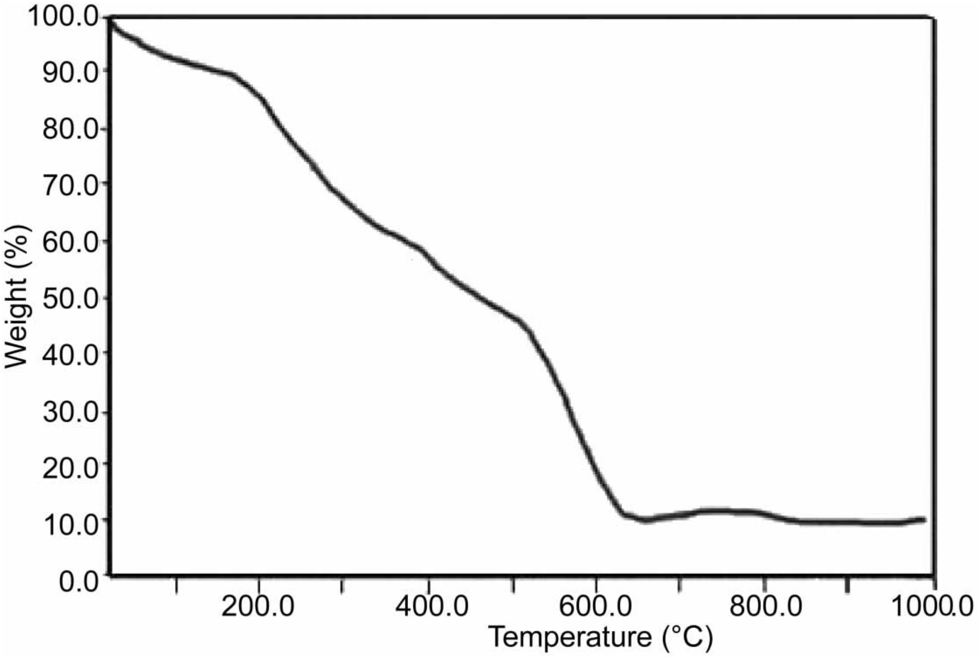

FIGURE 7 Thermogram of humic acids.

can be stabilised by organo–mineral associations, while the association of more labile polysaccharide-derived organic matter with minerals is weaker. We should, moreover, take into account that a part of the bulk TOC is involved in the process of humic substance formation, which is another mechanism of organic matter preservation.

Our results show that the TOC content decreases with depth at sites Y1 and Y3 while it is constant in the upper 10 cm in the Y5 sediment core and then decreases with increasing depth. This finding for the Y5 sediment core may be accounted for by a decreasing deposition of organic matter onto the sediment surface [31] which, associated with microbial degradation and mineralisation processes, could balance out the content of descending organic matter; on the other hand, the constant pattern could be ascribed to a fast sedimentation rate and/or to fine-grained composition of the sediment core.

The humic substance content follows the same pattern as TOC, decreasing with depth at sites Y1 and Y3 but remaining constant in the upper 17 cm of the Y5 sediment core and then decreasing with further depth.

The decrease with depth of humic and fulvic acid fractions, which represents the intermediate fraction in humification processes, indicates a shift from the freshly deposited organic matter on the sediment surface to more humified material (humin) with increasing distance from the sediment surface. Both degradation and condensation reactions can be involved in the humification of organic matter.

Significant microbial degradation of organic matter already occurs within the water column. However, peptides, carbohydrates, lipids and other high molecular weight organic compounds are sorbed on to metal oxides and mineral particles inside the water column, which protects them against degradation and leads to an enrichment of higher molecular weight molecules on the surface sediment. These biopolymers are

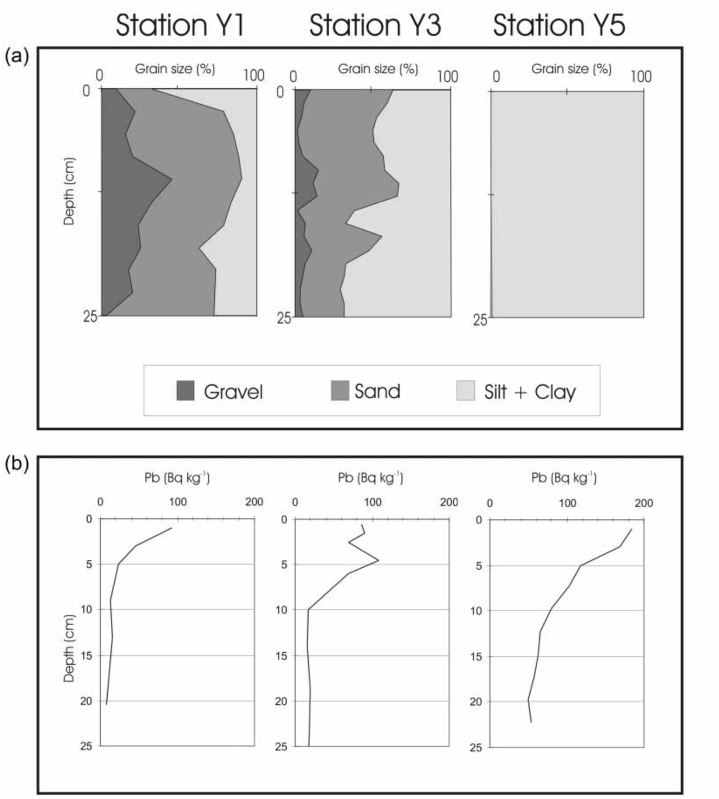

FIGURE 8 (a) Grain-size pattern and (b) ^{210}Pb profile at sites Y1, Y3 and Y5.

considered as possible precursors of aquatic humic material, especially in Antarctica where the source of organic matter is limited to microbial and algal biomass. The formation model of sedimentary humic substances assumes that these biopolymers are first degraded to small molecules and then repolymerised to produce humic and fulvic acids. These substances are the basic building blocks of humin (the insoluble fraction of humic substances).

Taken together, the elemental composition and spectroscopic analyses of humic substances are in agreement with the formation model via a degradation–recondensation process involving sedimentary humic substances proposed by Ishiwatary [13].

Our results show that C/N and H/C ratios decreased with depth at sites Y1 and Y3, thus confirming a decrease in peptide content and an increase in aromatic character relative to aliphatic, as shown by the results of spectroscopic analysis. Moreover, thermogravimetric analysis indicates that, as they travel downward, the humic acid molecules are subjected to a transformation process resulting in more condensed structures. These results confirm the hypothesis that humification processes have occurred. The "humification" process is marked in cores from sites Y1 and Y3 but not in the sites Y5 core, where no variations in the structural features of humic substances have been found. The results are probably due to a different rate of sedimentation among stations and/or different grain-size composition of sediments.

Sedimentary Interpretation

By comparing measured and expected ^{210}Pb inventories it is possible to draw some sedimentary inferences. At all the sites the excess ^{210}Pb inventories are higher than predicted. This indicates that some fine biological material deposited on the banks can be resuspended by strong currents and settles on the bottom of basins [32], thus contributing to increasing the ^{210}Pb inventory. This evidence also confirms the role that other authors [33,34] have assigned to ocean circulation as an important controller of sediment distribution in the Ross Sea.

The sediment accumulation rate can be calculated from ^{210}Pb activity–depth profiles using different models, each one representing a particular mechanism of ^{210}Pb and particle delivery to the bottom. Therefore, the choice of model is determined by the characteristics of the area investigated. In Antarctica, owing to the substantial absence of ice-free land and "non-marine" organic matter, the input of continental material to the sea is essentially due to the ice-rafted debris that is eroded from the old rock that constitutes the Antarctic craton. Nevertheless, ^{210}Pb can also be found in the atmosphere originating from ^{222}Rn emanating from the continent [35] and a small contribution of atmospheric aerosol/particles could be a possible additional sources for particulate material in seawater deposited during sedimentation on the ocean floor [36,37]. So, in a complex environment such as those represented by the studied sites, there is probably no simple model that describes the accumulation of ^{210}Pb and sediment.

Because of this we compared two different approaches: the CRS model [38] based on ^{210}Pb Constant Rate of Supply, and the CF–CS model [39] based on Constant Flux–Constant Sedimentation. The first model is probably the more reliable because the major contribution of ^{210}Pb to the Antarctic sediment comes from the decay of ^{226}Ra dissolved in the water column, which represents a constant source. In any case, the effect of mixing should be taken into account; we can assume that a CF–CS condition exists below the Surface Mixing Layer (SML), but if deep mixing is present the resulting accumulation rate may be overestimated. In any case the calculated rates should be considered as maximum limits. Sediment accumulation rates obtained with the two models are the same for site Y5 and comparable for the two other study sites.

The lowest apparent total accumulation rate for the study sites has been calculated for station Y1, with a value of $55\,\mathrm{g\,cm^{-2}\,ka^{-1}}$. Furthermore this sample shows the coarsest grain size (Fig. 8a). This is probably due to the strong continental input from ice and occurs during the melting phases. Using radiocarbon data measured in closer areas [18] to calculate the mixing layer of this area [32] we were able to observe that this site is least affected by reworking processes, especially those involving bioturbation. Therefore we can consider this apparent sedimentation rate as a real value.

The accumulation rate at station Y3, also calculated by ^{210}Pb inventories, is slightly higher than for site Y1, the apparent accumulation rate being $80\,\mathrm{g\,cm^{-2}\,ka^{-1}}$; unlike site Y1 the calculated mixing layer seems to be quite deep. For this reason the measured accumulation rate may be taken as a maximum value, and probably an overestimate by up to five times [32]. Therefore the real accumulation rate might range from 15 to $80\,\mathrm{g\,cm^{-2}\,ka^{-1}}$. A mean value would be around $47.5 \pm 32.5\,\mathrm{g\,cm^{-2}\,ka^{-1}}$. The data obtained could imply that, since the continental contributions are rather low because of the distance from the coast, the flux of primary productivity could also be low.

Furthermore, we cannot exclude processes of winnowing due to the presence of intense bottom currents that would remove the finest part of the sediment.

The apparent mass accumulation rate at site Y5 is 104 g cm^{-2} ka^{-1} and this is the highest value found in all study areas. Ravaioli *et al.* [24] and Labbrozzi *et al.* [32], calculated a deep mixing layer in this area and so this accumulation value can be considered an overestimate. Applying the reliable correction values used for previous site we obtained a more correct estimate ranging from 21 to 104 mg cm^{-2} ka^{-1} with a mean value of about 62 ± 42 mg cm^{-2} ka^{-1}. We can thus assume that this site is characterized by the highest accumulation rate of the three sites discussed in this paper.

In this site focussing processes of material from near morphological relics are also very consistent [18]; fluxes from sediment collected in moored traps actually display strong bottom sediment resuspension processes [39].

CONCLUSION

The results obtained from the organic carbon and humic substance content profiles and from the structural characterization of humic material indicated that the input and transformation processes of organic matter are different and the accommodation rate follows the order Y5 > Y1 > Y3. The Y5 site is found to be characterized by the highest "preservation" of organic matter, probably because of the highest sedimentation rate and/or the finest grain size. Sites Y1 and Y3 showed less marked differences and are characterized by degradation and humification processes involving bulk organic matter. Moreover, Y3 seems to be characterized by the lowest degree of preservation of organic bulk, probably associated with the lower accumulation rate.

The sedimentological data confirmed these findings. Indeed, the three study sites are different in grain size and composition. Site Y1 is affected by high continental input (coarser than other stations) because it is a coastal site. Conversely Y5 has the finest sample.

^{210}Pb depth distribution in the study areas leads to the calculation of apparent sediment accumulation ranging between 15 and 104 mg cm^{-2} yr^{-1}.

The highest calculated accumulation rate is at site Y5 and the lowest seems to be at Y1. But uncertainty remains concerning the real values for each site, owing to the bioturbation processes that are present at sites Y3 and Y5. The order based on the mean sedimentation rate is Y5 > Y1 > Y3. The overall interpretation of sedimentological data is quite consistent with that suggested by humic substance analysis.

We could conclude that the humic substances could be utilised as indicators for predicting sedimentological parameters. Nevertheless, further studies of different sites could be useful in order to generalize this finding.

Acknowledgements

The authors are indebted to G. Marozzi and E. Lipparini for box core sampling. We are also grateful to E. Lipparini and L. Labbrozzi for ^{210}Po extraction, G. Marozzi for X-ray analyses and F. Ravaioli and M. Mengoli for grain-size analyses. This work was supported by the National Programme for Antarctic Research, section 2c.4: Evolution and biogeochemical cycles of contaminants and section 2a.3: Glaciology and Paleoclimate, and by the Italian Ministry of the University and

Scientific and Technological Research (MURST, COFIN 2000, Project prot. MM03247343_003). This is contribution No. 1379 of the Istituto di Geologia Marina del CNR, Bologna.

References

[1] J.J. Middelburg, T. Vlug and F.J.W.A. Van Der Nat, *Global Planet. Change*, **8**, 47–58 (1993).

[2] J.I. Hedges and R.G. Keil, *Marine Chem.*, **49**, 81–115 (1995).

[3] S. Hulth, A. Tangberg, A. Landen and P.O.J. Hall, *Deep-Sea Res. I*, **44**, 955–981 (1997).

[4] J.I. Hedges, G. Eglinton, P.G. Hatcher, D.L. Kirchman, C. Arnosti, S. Derenne, R.P. Evershed, I. Kogel-Knabner, J.W. de Leeuw, R. Littke, W. Michaelis and J. Rulkotter, *Org. Geochem.*, **31**, 945–958 (2000).

[5] J.I. Hedges and J.M. Oades, *Org. Geochem.*, **27**, 319–361 (1997).

[6] R.V. Tyson, *Org. Geochem.*, **32**, 333–339 (2001).

[7] J.D.H. Van Heemst, S. Peulve and J.W. De Leeuw, *Org. Geochem.*, **24**, 629–640 (1996).

[8] P.A. Meyers, *Org. Geochem.*, **27**, 213–250 (1997).

[9] R.T. Nguyen and H.R. Harvey, *Geochim. Cosmochim. Acta*, **65**, 1467–1480 (2001).

[10] T. Miyajima, H. Ogawa and I. Koike, *Geochim. Cosmochim. Acta*, **65**, 1455–1466 (2001).

[11] Y. Zegouagh, S. Derenne, C. Largeau, P. Bertrand, M.A. Sicre, A. Saliot and B. Rousseau, *Org. Geochem.*, **30**, 83–99 (1999).

[12] J.I. Hedges, In: F.H. Frimmel and R.F. Christman (Eds.), *Humic Substances and thei Role in the Environment*, pp. 45–58. Dahlem Konferenzes, West Berlin (1988).

[13] R. Ishiwatary, *Marine Chem.*, **39**, 151–166 (1992).

[14] F.J. Stevenson, *Humus Chemistry, Genesis, Composition, Reactions*, 2nd Edn. J. Wiley & Sons, New York (1994).

[15] D.M. McKnight and G.R. Aiken, In: D.O. Hessen and L.J. Tranvik (Eds.), *Aquatic Humic Substances: Ecology and Biogeochemistry*, pp. 259–284. Springer, Berlin (1998).

[16] P.A. Meyers and R. Ishiwatary, *Org. Geochem.*, **20**, 867–900 (1993).

[17] S. Shipp, J. Anderson and E. Domack, *Geol. Soc. Am. Bull.*, **111**, 1486–1516 (1999).

[18] M. Frignani, F. Giglio, L. Langone and M. Ravaioli, *Annal. Glaciology*, **27**, 697–703 (1998).

[19] M. Schnitzer and S.U. Khan, *Humic Substances in the Environment*. Marcel Dekker, New York (1972).

[20] E.M. Thurman and R.L. Malcolm, *Environ. Sci. Technol.*, **15**, 463–466 (1981).

[21] N. Calace, F. De Paolis, F. Minniti and B.M. Petronio, *Talanta*, **47**, 803–809 (1998).

[22] M. Frignani and L. Langone, *Continental Shelf Res.*, **11**, 525–542 (1991).

[23] S.L. Harden, D.J. DeMaster and C.A. Nittrouer, *Marine Geol.*, **103**, 69–97 (1992).

[24] M. Ravaioli, M. Frignani, M.C. Cambi, L. Labbrozzi and L. Langone, In: G. Spezie and G.M.R. Manzella (Eds.), *Oceanography of the Ross Sea "Antarctica"*, pp. 209–222. Springer Verlag, Milan (1999).

[25] M.C. Gambi and S. Bussotti, *Polar Biol.*, **21**, 347–354 (1999).

[26] D.J. DeMaster, O. Ragueneau and C.A. Nittrouer, *J. Geophys. Res.*, **101**, 501–518 (1996).

[27] L. Langone, M. Frignani, L. Labbrozzi and M. Ravaioli, *J. Marine Syst.*, **17**, 459–470 (1998).

[28] M.W.I. Schmidt, H. Knicker and I. Kogel-Knabner, *Org. Geochem.*, **31**, 727–734 (2000).

[29] L.M. Mayer, *Chem. Geol.*, **114**, 3–4 (1994).

[30] L.M. Mayer, *Geochim. Cosmochim. Acta*, **58**, 1271–1284 (1994).

[31] A. Kappler, R. Ji, B. Schink and A. Brune, *Org. Geochem.*, **32**, 3–10 (2001).

[32] L. Labbrozzi, L. Langone, M. Frignani and M. Ravaioli, *Proceedings of 12th AIOL Congress*, pp. 121–130 (1998).

[33] J.B. Anderson, C.F. Brake and N.C. Myers, *Marine Geol.*, **57**, 295–333 (1984).

[34] R.B. Dunbar, J.B. Anderson, E.W. Domaci and S.S. Jacobs, In: S.S. Jacobs (Ed.), *Oceanography of the Antarctic Continental Shelf*, Vol. 43, pp. 291–312. Antarctic Research Series (1985).

[35] M. Baskaran, C.H. Coleman and P.H. Santschi, *J. Geophys. Res.*, **98**, 20555–20571 (1993).

[36] R. Cini, P. Desideri and L. Lepri, *Anal. Chim. Acta*, **291**, 329–340 (1994).

[37] G. Loglio, N.D. Innocenti, A.M. Stortini, G. Orlandi, U. Tesei, P. Mittner and R.L. Cini, *Anal. Chim. Acta*, **81**, 453–467 (1991).

[38] P.G. Appleby and F. Oldfield, *Catena*, **5**, 1–18 (1978).

[39] J.A. Robbins, In: J.O. Nriagu (Ed.), *The Biogeochemistry of Lead in the Environment*, pp. 285–393. Elsevier, Amsterdam (1978).

[39] L. Langone, M. Frignani, M. Ravaioli and C. Bianchi, *J. Marine Syst.*, **27**, 221–234 (2000).